

DUST ATTENUATION IN THE NEARBY UNIVERSE: A COMPARISON BETWEEN GALAXIES SELECTED IN THE ULTRAVIOLET AND IN THE FAR-INFRARED

V. BUAT,¹ J. IGLESIAS-PÁRAMO,¹ M. SEIBERT,² D. BURGARELLA,¹ S. CHARLOT,^{3,4} D. C. MARTIN,² C. K. XU,²
 T. M. HECKMAN,⁵ S. BOISSIER,⁶ A. BOSELLI,¹ T. BARLOW,² L. BIANCHI,⁵ Y.-I. BYUN,⁷ J. DONAS,¹
 K. FORSTER,² P. G. FRIEDMAN,² P. JELINSKI,⁸ Y.-W. LEE,⁷ B. F. MADORE,⁶ R. MALINA,¹
 B. MILLIARD,¹ P. MORISSEY,² S. NEFF,⁹ M. RICH,¹⁰ D. SCHIMINOVITCH,² O. SIEGMUND,⁸
 T. SMALL,² A. S. SZALAY,⁵ B. WELSH,⁸ AND T. K. WYDER²

Received 2004 April 2; accepted 2004 June 10; published 2005 January 17

ABSTRACT

We compare the dust attenuation properties of two samples of galaxies purely selected in the *Galaxy Evolution Explorer* (GALEX) near-ultraviolet band (NUV; 1750–2750 Å, $\lambda_{\text{mean}} = 2310$ Å) and in the far-infrared (FIR) at 60 μm. These samples are built using the GALEX and IRAS sky surveys over ~600 deg². The NUV-selected sample contains 95 galaxies detected down to NUV = 16 mag (AB system). Eighty-three galaxies in this sample are spiral or irregular, and only two of them are not detected at 60 μm. The FIR-selected sample is built from the IRAS PSCz survey, which is complete down to 0.6 Jy. Among the 163 sources, we select 118 star-forming galaxies that are well measured by IRAS; all but one are detected in NUV, and 14 galaxies are not detected in the far-ultraviolet band (FUV; 1350–1750 Å, $\lambda_{\text{mean}} = 1530$ Å). The dust-to-ultraviolet (NUV and FUV) flux ratio is calibrated to estimate the dust attenuation at both wavelengths. The median value of the attenuation in NUV is found to be ~1 mag for the NUV-selected sample, versus ~2 mag for the FIR-selected one. Within both samples, the dust attenuation is found to correlate with the luminosity of the galaxies. Almost all the NUV-selected galaxies and two-thirds of the FIR-selected sample exhibit a lower dust attenuation than expected from the tight relation found previously for starburst galaxies between dust attenuation and the slope of the ultraviolet continuum. The situation is reversed for the remaining third of the FIR-selected galaxies: their extinction is higher than that deduced from their FUV – NUV color and the relation for starbursts.

Subject headings: dust, extinction — galaxies: photometry — galaxies: stellar content — infrared: galaxies — ultraviolet: galaxies

1. INTRODUCTION

To quantify star formation activity in the universe, from low to high redshift or in individual galaxies, we need as accurate an estimate as possible of the recent star formation rate in galaxies. Among various potential estimators, the far-infrared and ultraviolet luminosities are commonly used. Both emissions are expected to come from young stars (see, e.g., Kennicutt 1998 and references therein). The ultraviolet light is emitted by young stars and is theoretically directly connected to the recent star formation rate. However, the use of ultraviolet emission to trace the star formation is largely hampered by the presence of dust, which absorbs and scatters the ultraviolet light; the far-infrared (FIR) emission is not affected by this limitation. In fact, the ultraviolet and FIR emission are com-

plementary: the ultraviolet light lost because of dust absorption is reemitted in the FIR by the dust. This energy budget has been used to derive a measure of the dust attenuation (Xu & Buat 1995; Meurer et al. 1999; Gordon et al. 2000). This attenuation is known to be very large in some objects, and even if it remains modest on average in the nearby universe (Xu & Buat 1995), it is crucial to correct the observed ultraviolet flux before making any quantitative interpretation.

In this Letter, we consider a galaxy sample selected in the *Galaxy Evolution Explorer* (GALEX) near-ultraviolet band (NUV; 1750–2750 Å, $\lambda_{\text{mean}} = 2310$ Å) for which most of the galaxies have been observed in the FIR. Because of its selection, this sample will be directly comparable to optically (ultraviolet rest-frame) selected samples at higher redshift. We derive the dust attenuation from a comparison between the FIR and the near- and far-ultraviolet (FUV; 1350–1750 Å, $\lambda_{\text{mean}} = 1530$ Å) emission and discuss variations of this attenuation with luminosity and FUV – NUV color of the galaxies. For comparison, we also build an FIR-selected sample of galaxies, most of these being detected in NUV. We perform the same analysis as for the NUV-selected sample.

A similar, pioneering work has already been performed over only 35 deg² and at a single ultraviolet wavelength (Iglesias-Páramo et al. 2004). Complementary approaches may consist in exploring variations of the FIR-to-ultraviolet ratio within single nearby galaxies (Boissier et al. 2005; Popescu et al. 2005).

2. THE SAMPLES

Here we briefly discuss how we select our samples. Galaxy distances are calculated from their redshift measurements taken

¹ Laboratoire d’Astrophysique de Marseille, BP 8, Traverse du Siphon, F-13012 Marseille Cedex 12, France; veronique.buat@oamp.fr.

² Space Astrophysics Laboratory, Mail Stop 405-47, California Institute of Technology, 1200 East California Boulevard, Pasadena, CA 91125.

³ Institut d’Astrophysique de Paris, CNRS, 98 bis boulevard Arago, F-75014 Paris, France.

⁴ Max-Planck-Institut für Astrophysik, Karl-Schwarzschild-Strasse 1, D-85748 Garching, Germany.

⁵ Department of Physics and Astronomy, Johns Hopkins University, 3400 North Charles Street, Baltimore, MD 21218.

⁶ Observatories of the Carnegie Institution of Washington, 813 Santa Barbara Street, Pasadena, CA 91101.

⁷ Center for Space Astrophysics, Yonsei University, Seoul 120-749, Korea.

⁸ Space Sciences Laboratory, University of California, Berkeley, 7 Gauss Way, Berkeley, CA 94720.

⁹ Laboratory for Astronomy and Solar Physics, Code 681, NASA Goddard Space Flight Center, Greenbelt, MD 20771.

¹⁰ Department of Physics and Astronomy, UCLA, Box 951547, Los Angeles, CA 90095.

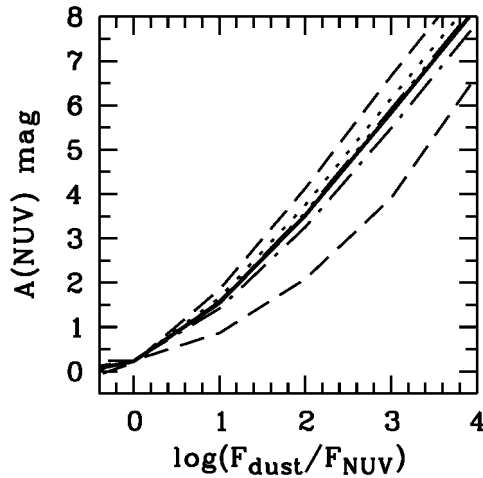


FIG. 1.—Predicted attenuation by dust in the *GALEX* NUV band as a function of the dust-to-NUV flux ratio. Various star formation rates are used: constant (dotted line), a 5 Myr old burst (upper short-dashed line), and exponential decreases with τ of 2 Gyr (lower short-dashed line), 4 Gyr (dot-dashed line) and 8 Gyr (solid line). The polynomial fit adopted in the paper (eq. [1]) is plotted with a solid line and closely follows the $\tau = 8$ Gyr model.

from the NASA/IPAC Extragalactic Database (NED), HyperLeda,¹¹ and the *IRAS* PSCz survey (Saunders et al. 2000), assuming $H_0 = 72 \text{ km s}^{-1} \text{ Mpc}^{-1}$. For very nearby galaxies (four sources), the distances were found in the literature. All magnitudes are expressed on the AB system.

Our NUV-selected sample, down to $\text{NUV} = 16 \text{ mag}$, is built from the first observations of the *GALEX* All-sky Imaging Survey (see Martin et al. 2005 and Morrissey et al. 2005 for details regarding the *GALEX* instrument and mission). We select only those frames with exposure times larger than or equal to 50 s; the resulting field covers 615 deg^2 . We perform photometry using the *GALEX* internal release IR0.2 calibration and apply a zero-point offset of $+0.039 \text{ mag}$ in FUV and -0.099 mag in NUV. We mask bright stars and galaxies that lie close to our targets. For each target, the sky background is measured by combining several individual nearby-sky regions. NUV fluxes are extracted using elliptical apertures enclosing the total fluxes. FUV magnitudes are measured within the same aperture.

NUV and FUV fluxes were first corrected for Galactic extinction using the Schlegel et al. (1998) dust maps and the Cardelli et al. (1989) extinction curve. A total of 95 sources brighter than $\text{NUV} = 16 \text{ mag}$ were then selected. We exclude objects whose ultraviolet flux can be contaminated by sources other than young stars, that is, early-type (two elliptical) and active galaxies (two Seyfert 1's, two Seyfert 2's, and one QSO). Most of the remaining 88 sources are late-type spirals.

We search for a detection at $60 \mu\text{m}$ for all 88 sources using the *IRAS* Faint Source Catalog (Moshir et al. 1992) and the Scan Processing and Integration Facility (SCANPI). Four galaxies were not observed by *IRAS*. All other sources but three are detected at $60 \mu\text{m}$. For the three nondetections, we adopt a conservative upper limit of 0.2 Jy at $60 \mu\text{m}$. Among the 81 galaxies with an *IRAS* detection, 22 are contaminated by cirrus or have close neighbors not resolved by *IRAS*. We discard these measures from the quantitative analysis of the FIR emission. We are thus left with 59 sources with an NUV flux and a flux at $60 \mu\text{m}$, and three NUV sources with only an upper limit at $60 \mu\text{m}$.

To construct the FIR-selected sample, we start with the *IRAS* PSCz catalog (Saunders et al. 2000), which is complete down to 0.6 Jy at $60 \mu\text{m}$; we take advantage of the optical identification of the *IRAS* sources to search for an NUV detection. We select 163 *IRAS* sources over 509 deg^2 detected at $60 \mu\text{m}$ with a reliability greater than 50% and not contaminated by cirrus; 144 targets also have a flux at $100 \mu\text{m}$, and the remainder have only upper limits. Among these 163 galaxies, 97 have a morphological type in NED or LEDA. We discard four elliptical or lenticular galaxies, three Seyfert 1's and five Seyfert 2's, and 33 galaxies that have close neighbors not resolved by *IRAS*. We are thus left with 118 galaxies. NUV and FUV photometry are performed following the same prescription as for the NUV-selected sample.

All galaxies but one are detected in NUV (signal-to-noise ratio larger than 3). Fourteen galaxies are not detected in FUV. For the nondetections in NUV or FUV, upper limits are estimated corresponding to a signal-to-noise ratio of 3.

3. DUST ATTENUATION AT ULTRAVIOLET WAVELENGTHS

3.1. Modeling

It has been shown (Buat & Xu 1996; Meurer et al. 1999; Gordon et al. 2000) that for ultraviolet measurements up to 2000 \AA , the dust-to-ultraviolet flux ratio is a robust tracer of dust attenuation in star-forming galaxies regardless of the details of the extinction mechanisms (dust/star geometry, dust properties). Hereafter F_{dust} refers to the total dust emission and F_{FUV} and F_{NUV} are defined for each *GALEX* band as νF_ν , where F_ν is expressed in $\text{W m}^{-2} \text{ Hz}^{-1}$.

Since the NUV band of *GALEX* lies at wavelengths longer than 2000 \AA , we must test the reliability of the $F_{\text{dust}}/F_{\text{NUV}}$ ratio in estimating the dust attenuation for various scenarios of star formation. With this aim, we use the population synthesis code PEGASE (Fioc & Rocca-Volmerange 1997) under different hypotheses about the star formation rate (SFR; see Fig. 1). The amount of dust emission is obtained by adding all the stellar emission absorbed by the dust. We tried different configurations for the dust attenuation: Calzetti's screenlike attenuation law (Calzetti et al. 2000), a homogeneous mixture of dust and stars in a slab geometry with a Galactic or an LMC stellar extinction law (Buat & Xu 1996), and a clumpy medium (Calzetti et al. 1994). We also include the time-dependent scenario proposed by Charlot & Fall (2000). Within this framework, we develop another bivariate model in which the attenuation of the light from stars younger than 10^7 yr follows the Calzetti law whereas older stars are supposed to be homogeneously mixed with the dust or to be distributed in a clumpy medium. All these models give very similar results for a given star formation history, with a dispersion lower than 5%. In particular, the exact form of the extinction curve (with or without a 2175 \AA bump) does not affect the results. Each curve plotted in Figure 1 is the average over all these scenarios for a specific star formation rate. Similar plots are found with the FUV flux instead of the NUV one. Only the exponentially decreasing SFR with $\tau = 2 \text{ Gyr}$ leads to a much lower attenuation for a given dust-to-NUV flux ratio: the dust heating by old stars becomes important, and only a fraction of the dust emission is related to the ultraviolet absorption. Such a steep decrease of the SFR is typical of elliptical or lenticular galaxies (Gavazzi et al. 2002). All the other star formation scenarios lead to a relative error lower than 20%. The calibration holds for both *GALEX* bands, and the $F_{\text{dust}}/F_{\text{NUV}}$ will be used to estimate the dust attenuation, since more galaxies are detected in NUV than in FUV.

¹¹ See <http://leda.univ-lyon1.fr>.

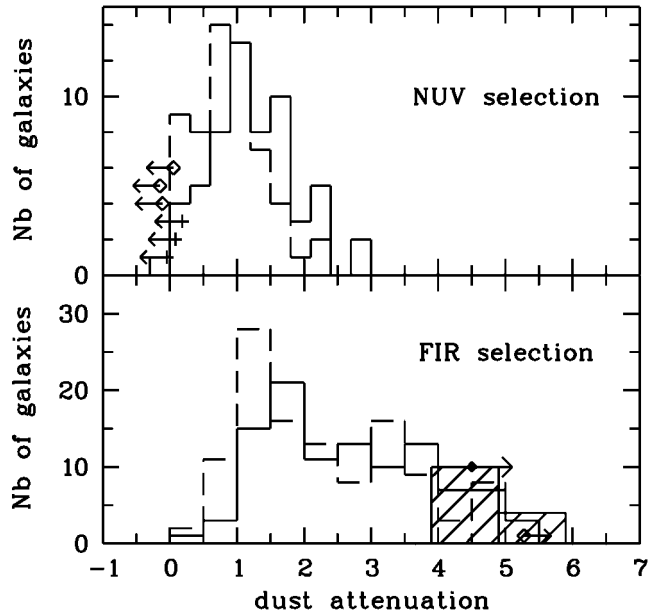


FIG. 2.—Histograms of the dust attenuation: *solid lines*, A_{FUV} ; *dashed lines*, A_{NUV} . *Top*: The NUV-selected sample; the upper limits are plotted with plus signs and left arrows for the FUV band and diamonds and left arrows for the NUV band. *Bottom*: The FIR-selected sample; the dashed histogram represents the lower limits in A_{FUV} , and the only lower limit in A_{NUV} is plotted with a diamond and right arrow.

We performed polynomial fits on our models, excluding the curves with $\tau = 2$ Gyr because the FIR and NUV selections focus on active star-forming galaxies and we exclude elliptical and lenticular galaxies from the study:

$$A_{NUV} = -0.0495x^3 + 0.4718x^2 + 0.8998x + 0.2269, \quad (1)$$

where $x = \log(F_{dust}/F_{NUV})$, and

$$A_{FUV} = -0.0333y^3 + 0.3522y^2 + 1.1960y + 0.4967, \quad (2)$$

where $y = \log(F_{dust}/F_{FUV})$. These fits are fully consistent with the mean relations between the dust attenuation and the dust-to-ultraviolet flux ratio for both *GALEX* bands proposed by Kong et al. (2004) and S. Charlot & J. Brinchmann (2004, private communication) for similar star formation histories.

3.2. The Amount of Dust Attenuation

Before estimating the attenuation with the above formulae, we need to estimate the total dust emission. For the galaxies observed at 60 and 100 μm , we calculate this total following Dale et al. (2001). Three galaxies from the NUV-selected sample were not detected at 100 μm ; we use the mean value of the F_{60}/F_{100} ratio found for the sample galaxies detected at both wavelengths to estimate their flux at 100 μm . The mean bolometric corrections $\langle F_{dust}/F_{FIR} \rangle$ are equal to 2.8 ± 1.1 and 2.4 ± 1.1 for the NUV- and FIR-selected samples, respectively (the FIR flux is defined between 40 and 120 μm ; Helou et al. 1988). These values are intermediate between those found for starbursts and cirrus-dominated galaxies (Calzetti et al. 2000; Rowan-Robinson 2003). In the NUV-selected sample, the median values of the dust attenuation in *GALEX* bands are found to be $0.8^{+0.3}_{-0.3}$ mag in NUV and $1.1^{+0.4}_{-0.5}$ mag in FUV.

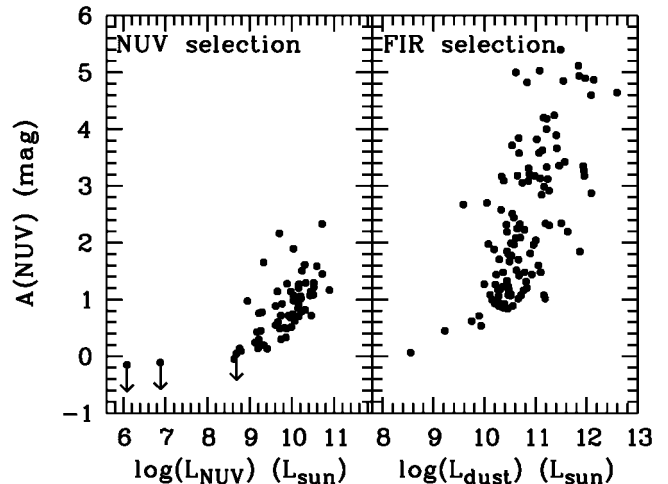


FIG. 3.—Dust attenuation in the *GALEX* NUV band vs. the luminosity of the galaxies. *Left*: The NUV-selected sample; the luminosity is the NUV value corrected for dust attenuation. *Right*: The FIR-selected sample; the luminosity is the total dust luminosity.

In the FIR-selected sample, the median values found for the dust attenuation are larger: $2.1^{+0.9}_{-1.1}$ mag in NUV and $2.9^{+1.1}_{-1.3}$ mag in FUV. The galaxies not detected in FUV have a dust attenuation larger than ~ 5 mag, in agreement with the large attenuations (≥ 4 mag) found in the NUV band. The histograms of the attenuations are given in Figure 2.

In Figure 3, the dust attenuation in the NUV band is compared with the intrinsic luminosity of the galaxies expected to be the best measurement of the recent star formation rate: the NUV luminosity corrected for the extinction for the NUV-selected sample (*left*) and the dust luminosity for the FIR-selected sample (*right*). In both cases the dust attenuation is found to increase with the luminosity. This result is consistent with findings of an increase of dust attenuation with SFR in nearby galaxies (Wang & Heckman 1996; Hopkins et al. 2001). Vijh et al. (2003) proposed a law between the extinction and the luminosity at 1600 \AA for bright Lyman break galaxies at $z > 2$; extrapolation of this law to fainter objects predicts lower attenuations than those found for our NUV-selected sample. This effect might be attributed to some evolution of the dust attenuation with redshift.

3.3. Mean Dust Attenuation in the Local Universe

We can compare the dust attenuation found in our samples with the mean dust attenuation estimated from the FIR and NUV (or FUV) luminosity densities (see, e.g., Buat et al. 1999). With this aim we calculate the ratio of the FIR and NUV (FUV) luminosity densities and translate it to a mean dust attenuation. The FIR density is taken from Saunders et al. (1990): $\rho_{FIR} = 3.9 \times 10^7 L_{\odot} \text{ Mpc}^{-3}$ with $h = 0.7$. The NUV and FUV luminosity densities are derived from the new *GALEX* data (Wyder et al. 2005): $\rho_{NUV} = 1.8 \times 10^7 L_{\odot} \text{ Mpc}^{-3}$ and $\rho_{FUV} = 1.9 \times 10^7 L_{\odot} \text{ Mpc}^{-3}$. Adopting $\langle F_{dust}/F_{FIR} \rangle \approx 2.5$, we obtain $\rho_{dust}/\rho_{NUV} \approx \rho_{dust}/\rho_{FUV} \approx 5.5$, which translates to dust attenuations of 1.1 and 1.6 mag in NUV and FUV, respectively. These mean values are intermediate between those found with our FIR and NUV selection but closer to the dust attenuation found for the NUV-selected galaxies. Therefore, as far as the dust attenuation is concerned, an NUV selection seems to be

more representative of the mean galaxy properties in the local universe than an FIR selection.

3.4. FUV – NUV Color and Dust Attenuation

Bell (2002) and, more recently, Kong et al. (2004) showed that the slope of the ultraviolet continuum (which can be traced by the FUV – NUV color) is not a reliable tracer of the dust attenuation in galaxies that are not experiencing a strong starburst. In Figure 4, we plot the FUV – NUV color against the dust-to-FUV flux ratio for the NUV-selected and the FIR-selected galaxies. We keep only galaxies brighter than 20 mag in NUV and FUV in order to have a photometric error in each band lower than or equal to 0.15 mag. Almost all the NUV-selected galaxies and a large fraction of the FIR-selected ones lie below the curve, followed by starburst galaxies (Meurer et al. 1999; Kong et al. 2004): they exhibit a lower $F_{\text{dust}}/F_{\text{FUV}}$ (i.e., a lower attenuation) than do starbursts for a given FUV – NUV color, as already found for nonstarbursting galaxies. Kong et al. (2004) explain this behavior with a variation of the ratio of present to past average SFR: our data are roughly consistent with a ratio varying from 1 to 0.1. About one-third of the FIR-selected galaxies lie above the curve valid for starburst galaxies: their dust attenuation is larger than that expected from the FUV – NUV color. This trend is similar to that for ultraluminous infrared galaxies (ULIRGs; Goldader et al. 2002), although the dust attenuations found here are not as large as for the ULIRGs. The FUV – NUV color therefore seems unable to trace the dust attenuation in these galaxies.

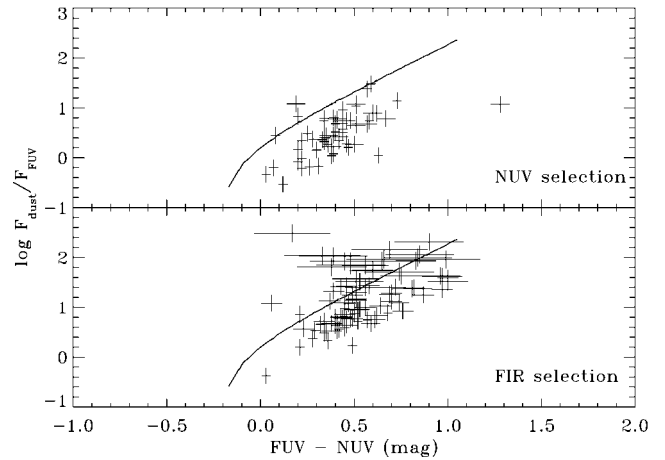


FIG. 4.—The $\log(F_{\text{dust}}/F_{\text{FUV}})$ vs. FUV – NUV color for the NUV- and FIR-selected samples. The solid line is the mean relation expected for starburst galaxies (Kong et al. 2004). The error bars were estimated assuming 15% uncertainty for the *IRAS* fluxes and 40% uncertainty for the $\langle F_{\text{dust}}/F_{\text{FIR}} \rangle$ ratio; the errors on the FUV and NUV fluxes were assumed to be Poissonian.

GALEX is a NASA Small Explorer, launched in 2003 April. We gratefully acknowledge NASA's support for construction, operation, and science analysis for the *GALEX* mission, developed in cooperation with the Centre National d'Etudes Spatiales of France and the Korean Ministry of Science and Technology.

REFERENCES

- Bell, E. F. 2002, *ApJ*, 577, 150
 Boissier, S., et al. 2005, *ApJ*, 619, L83
 Buat, V., Donas, J., Milliard, B., & Xu, C. 1999, *A&A*, 352, 371
 Buat, V., & Xu, C. 1996, *A&A*, 306, 61
 Calzetti, D., Armus, L., Bohlin, R. C., Kinney, A. L., Koornneef, J., & Storchi-Bergmann, T. 2000, *ApJ*, 533, 682
 Calzetti, D., Kinney, A. L., & Storchi-Bergmann, T. 1994, *ApJ*, 429, 582
 Cardelli, J. A., Clayton, G. C., & Mathis, J. S. 1989, *ApJ*, 345, 245
 Charlot, S., & Fall, S. M. 2000, *ApJ*, 539, 718
 Dale, D. A., Helou, G., Contursi, A., Silbermann, N. A., & Kolhatkar, S. 2001, *ApJ*, 549, 215
 Fioc, M., & Rocca-Volmerange, B. 1997, *A&A*, 326, 950
 Gavazzi, G., Bonfanti, C., Sanvito, G., Boselli, & Scodreggio, M. 2002, *ApJ*, 576, 135
 Goldader, J. D., Meurer, G., Heckman, T. M., Seibert, M., Sanders, D. B., Calzetti, D., & Steidel, C. C. 2002, *ApJ*, 568, 651
 Gordon, K. D., Clayton, G. C., Witt, A. N., & Misselt, K. A. 2000, *ApJ*, 533, 236
 Helou, G., Khan, I. R., Malek, L., & Boehmer, L. 1988, *ApJS*, 68, 151
 Hopkins, A. M., Connolly, A. J., Haarsma, D. B., & Cram, L. E. 2001, *AJ*, 122, 288
 Iglesias-Páramo, J., Buat, V., Donas, J., Boselli, A., & Milliard, B. 2004, *A&A*, 419, 109
 Kennicutt, R. C., Jr. 1998, *ARA&A*, 36, 189
 Kong, X., Charlot, S., Brinchmann, J., & Fall, S. M. 2004, *MNRAS*, 349, 769
 Martin, D. C., et al. 2005, *ApJ*, 619, L1
 Meurer, G. R., Heckman, T. M., & Calzetti, D. 1999, *ApJ*, 521, 64
 Morrissey, P., et al. 2005, *ApJ*, 619, L7
 Moshir, M., et al. 1992, Explanatory Supplement to the *IRAS* Faint Source Survey, Version 2 (Pasadena: JPL)
 Popescu, C. C., et al. 2005, *ApJ*, 619, L75
 Rowan-Robinson, M. 2003, *MNRAS*, 344, 13
 Saunders, W., Rowan-Robinson, M., Lawrence, A., Efstathiou, G., Kaiser, N., Ellis, R. S., & Frenk, C. S. 1990, *MNRAS*, 242, 318
 Saunders, W., et al. 2000, *MNRAS*, 317, 55
 Schlegel, D. J., Finkbeiner, D. P., & Davis, M. 1998, *ApJ*, 500, 525
 Vijh, U. P., Witt, A. N., & Gordon, K. D. 2003, *ApJ*, 587, 533
 Wang, B., & Heckman, T. M. 1996, *ApJ*, 457, 645
 Wyder, T. K., et al. 2005, *ApJ*, 619, L15
 Xu, C., & Buat, V. 1995, *A&A*, 293, L65